

# Applications of the Electron Probe Microanalyser

By J. Philibert and C. Crussard

THE MICROANALYSER with electronic probe invented by R. Castaing and constructed by the Office Nationale d'Etude et Recherches Aéronautiques is intended for making quantitative elementary analyses at points in massive specimens, metallic or otherwise (see Fig. 1). The apparatus itself has been described elsewhere<sup>1</sup>; the principle is, briefly, that an extremely fine pencil of electrons (the electron probe) is directed at the specimen and the characteristic X-rays emitted by the specimen under the impact of the electrons are analysed. The apparatus therefore consists essentially of an electron optical system and an X-ray spectrometer; a mirror-objective microscope permits normal observations of the specimen, prepared as usual for metallography, to be made.

The extent of the 'resolving power' of the apparatus is  $2\mu$  in length (this being the minimum diameter of the region analysed) and  $1-2\mu$  in depth. All elements heavier than chlorine (atomic No. 17) can be determined, and the extension to elements down to aluminium or magnesium is being studied. However, the analysis of very light elements like carbon, nitrogen, and oxygen is not at present envisaged.

The error in analysis is about  $\pm 1\%$  for elements in concentrations greater than  $0.5\%$ , which excludes analysis of traces (concentrations below  $0.1\%$ ).

The present paper gives the results of tests made since the microanalyser has been in service at IRSID. These experiments were made mainly to assess rapidly the scope of the apparatus in the various branches of metallurgical research, namely, the study of ores (distribution of iron in oolites), of oxide scales in mild steel (selective oxidation), and of minor segregation of Ni, Cr, and Mn in steels having a banded structure. The paper continues with results obtained in phase-transformation studies: the identification of precipitates (oxides, carbides, sulphides, etc.) and the

## SYNOPSIS

The Castaing-ONERA Electron Probe Microanalyser has been in service for a short time at IRSID. The instrument permits elementary point analyses to be made (over an area of  $1-2\mu$  dia.) of all elements of atomic number greater than 17, with an error of  $1\%$ . The results of the first experiments made at IRSID to explore its possibilities for ferrous metallurgical investigation are reported, from the study of ores (oolite), oxide scales, and segregation bands in steels, to metallographical studies (phase transformations, analysis and identification of phases, and studies of diffusion). 1292

analysis of different constituents—measurements from which it is easy to work out constitutional diagrams. The paper ends with a report of some studies on diffusion in various metals and alloys.

## STUDY OF IRON ORES

The microanalyser can be used for the study not only of metals but also of insulators by a special surface treatment (metallization of the surface to a thickness of 300 or 400 Å). Examination has been made of oolites extracted from Lorraine ore (Sainte-Barbe brown ore), enveloped in plastic, and polished (see Fig. 2). Determinations of iron have been made in the core and in the various concentric aureoles of the oolite. Table I gives some typical results.

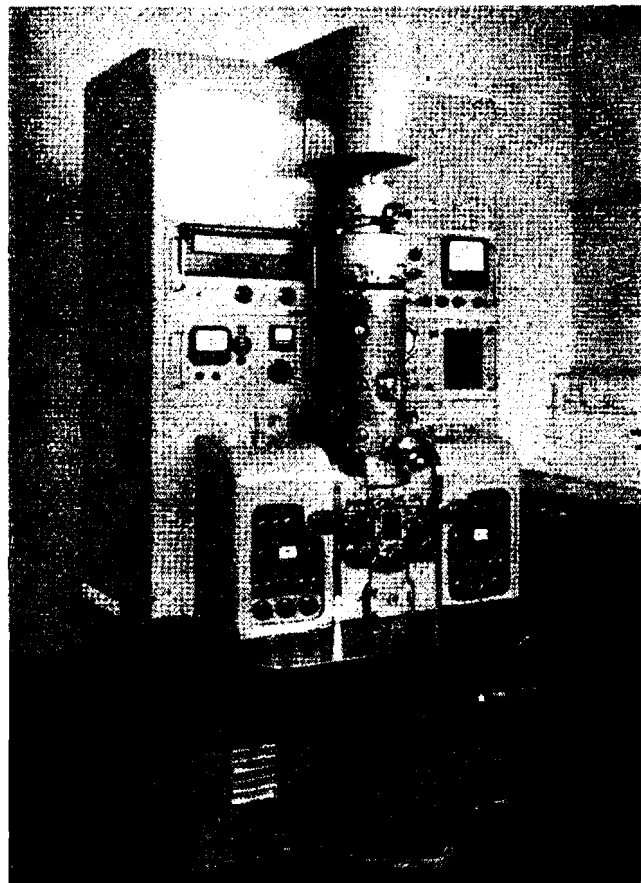


Fig. 1—Electron probe microanalyser

Table I

### EXAMINATION OF OOLITIC ORE

Oolite No.	Part Analysed	Fe, %
1	Central core	50.5
	Very black zones	43.5-44.5
	White zones	48.5-49.5
	Grey zones	45.5-46.5
2 (Fig. 2)	Central core	52.5
	Very black zones	42.5
	Grey-black zones	45.5-46.5
	White zones	48-49

Note: The manganese concentration is too low for a detailed study but it seems that the zones richest in iron are always richest in manganese.

The usual approximation is not accurate enough for determining the contents of ores from measurements of line intensities. If  $k_A$  is the intensity ratio for a strong line ( $K\alpha_1$  in the present case), emitted by an element  $A$  in the 'alloy' studied and by the pure element (standard or reference specimen), to a first approximation

$$C_A = k_A (C_A = \text{concentration of } A) \dots \dots \dots (1)$$

Castaing<sup>1</sup> has shown that a second approximation is

$$C_A = \frac{k_A}{(1 - a)k_A + a} \dots \dots \dots (2)$$

where  $a$  is a coefficient which is a function of the different absorption effects for electrons of the various elements of the alloy.

For alloys of elements of neighbouring atomic numbers,  $a$  can be taken as unity and equation (2) reduces to equation (1). In the present case, where the alloy contains about 50% of light elements (oxygen in particular), equation (2), which is hyperbolic, must be used. But  $a$  cannot be worked out as a function of the Lenard coefficients for the elements in the 'alloy'; it is simplest to determine it empirically. To do this, samples of hematite have been prepared in the same way as the oolites; under these conditions for an iron concentration of 0.70, it is found that  $k_{Fe} = 0.65$ , and  $a$  is deduced to be about 0.80. This is the value of  $a$  with which the values in Table I for the iron concentration have been calculated, via equation (2).

It is intended to confirm this value of  $a$  with other specific compounds having various iron contents, e.g. goethite and siderite, and to see if an identical value of  $a$  is obtained from pyrites.

**SELECTIVE OXIDATION DURING THE FORMATION OF SCALES**

Billets reheated in an oil-fired furnace exhibit surface oxide scales of complex structure, the various constituents of which can be investigated in a micro-

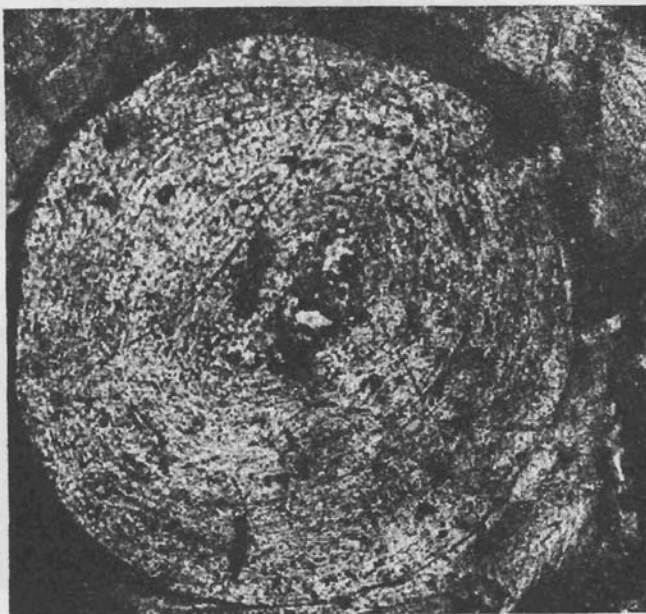
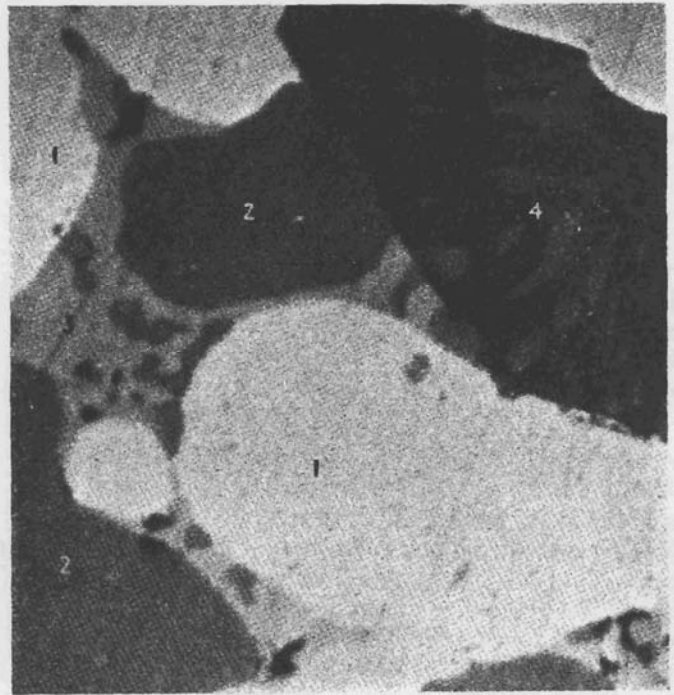


Fig. 2—Mechanically polished oolite extracted from a Sainte-Barbe ore  $\times 180$



1: Metal; 2: FeO; 3: FeS; 4: Silicate

Fig. 3—Mechanically polished oxide scale in O.H. steel  $\times 1200$

graphic section with the microanalyser. In particular studies have been made of billets of O.H. medium-hard steel of composition: C 0.4%, Mn 0.6%, Si 0.31%, Ni 0.22%, and Cu 0.14%. The micrograph of the internal part of this scale (Fig. 3) shows the existence of four phases. The results of the analyses given in Table II enable the phases to be identified from their content of Fe (+ Mn), since it is known almost in advance what phases will be encountered.

There is a considerable enrichment in Ni of the metal present as a core surrounded by oxides, sulphides, and silicates, in which no trace of this metal could be detected. In the same way, there is segregation of Cu, which also appears in the sulphide, but is not detectable in the oxide or silicate. Conversely, manganese appears mainly in the silicate.

**SEGREGATION OF Cr, Ni, AND Mn**

In steels having a marked banded structure, a minor segregation has been detected, fairly low for Cr and Ni in an Ni-Cr-Mo steel, but much stronger for Mn in a tyre steel.

**Segregation of Ni and Cr**

The steel investigated was of the following percentage composition:

C	Mn	Si	S	P
0.16	0.46	0.2	0.013	0.008
Ni	Cr	Mo	Cu	As
3.02	1.02	0.26	0.12	0.055

This steel exhibits well-marked segregation bands after tempering at 850° C for 30 min. It was studied after tempering for 28 h at 600° C; there is an alternation of ferritic and pearlitic zones after etching with nital (Fig. 4). The contents of Ni and Cr in these zones are given in Table III.

The variations of nickel are quite low: not more than 20% in relative value. The variations in chromium content are also small, and hardly more

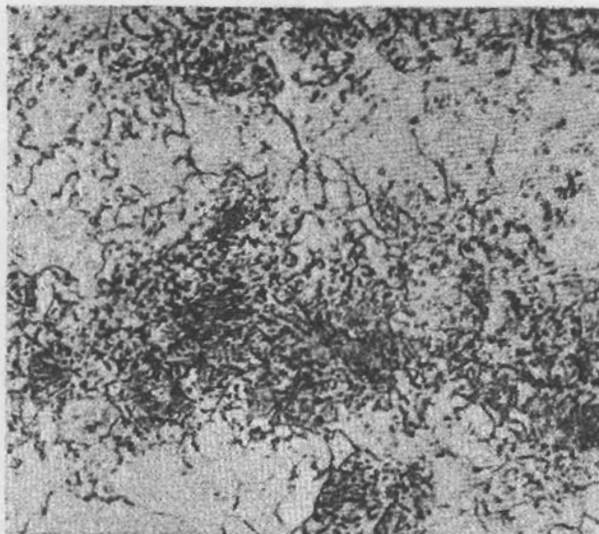


Fig. 4—Steel 16NCD13, austenitized at 850° C and tempered for 28 h at 600° C. Etched with nital  $\times 540$

than the concentration heterogeneity on the scale studied. These variations can always be revealed by making analyses with the electron probe at various points across two adjacent bands.

#### Segregation of Manganese

An apparently considerable segregation of manganese in hot-worked steels has already been revealed by microradiography<sup>2</sup>; this segregation more or less follows the fibre texture. But the resolving power of microradiography is not high enough to indicate whether the manganese in question is present as (sulphide?) inclusions and gives no idea of the magnitude of the segregation. These questions can be answered with the microanalyser. A tyre steel containing 0.55% C, 1.05% Mn, 0.026% S, 0.3% Si, 0.020% P was studied. Etching with Comstock's reagent (see Fig. 5), which reveals phosphorus segregation (the black zones are low in phosphorus), produces a typical segregation-band pattern. Some sulphides may be observed in the white bands. The results of analyses of Mn and Fe at different points are shown in Table IV.

These analyses show that, independently of segregation of manganese due to the presence of sulphides,

Table II  
EXAMINATION OF MILD-STEEL SCALES

Area Analysed	Fe	Mn	Ni		Phase	
1: white	96	0	3	0.75	100	Metal
2: mouse grey	77	0.5	Nil	Nil	77-77.5	FeO
3: yellow-grey	62	0.5	Nil	0.8	63-63.5	FeS
4: grey-black	52	1-1.5	Nil	Nil	53	Silicate

Table III  
ANALYSIS OF Ni-Cr-Mo STEEL

Zone Analysed	Ni, %	Cr, %
White	2.70-2.80	0.8-0.9
Grey	2.9-3.1	1
Grey-white	3.2	1.2

Table IV  
Mn AND Fe ANALYSES

Zone Studied	White	Grey	Black	Sulphide
Mn, %	1.4	0.9-1.1	0.7	42.5
Fe, %				20.5

there is a considerable segregation in the body of the metal itself, in the same zones as those in which phosphorus segregates. A subject for further study is whether this segregation is simultaneous or whether one controls the other.

#### TRANSFORMATIONS IN STEELS—IDENTIFICATION AND STUDY OF CONSTITUTION DIAGRAMS

It has already been seen, from the study of billet scales, that the microanalyser can be used to identify compounds of stoichiometric composition. Later examples are given of similar identifications of sulphides, carbides, etc. Local analysis of two phases present in equilibrium enables constitution diagrams to be worked out with a much smaller number of alloys than do the customary methods.

#### Sulphides

Local analyses were made on two types of sulphides found in casting skins on cast iron (Fig. 6): the yellowish-grey hexagonal 'iron sulphide' and the mouse-grey cubic 'manganese sulphide.' The results are given in Table V; the total Fe + Mn is always 63%, which corresponds satisfactorily with the stoichiometric composition of the sulphide and at the same time identifies it.

Note that the iron sulphide scarcely dissolves any manganese, while the 'manganese sulphide' sometimes contains more iron than manganese.

#### Carbides

In high-alloy steels, the microprobe allows the

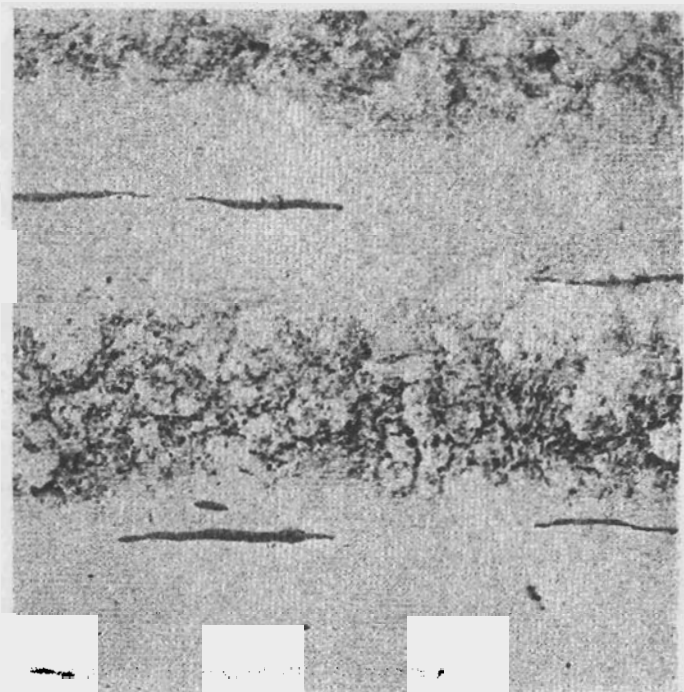


Fig. 5—Strip steel containing 1% Mn, etched with Constock's reagent  $\times 350$

**Table V**  
**ANALYSES OF SULPHIDES ON CAST IRON**

Zone Analysed	Mn	Fe	Total
Yellowish-grey	2.3	60-61	63
Mouse-grey	43	20	63
"	36	27	63
"	25.5	37.5	63

evolution of carbides to be followed during high-temperature heat-treatment. Specimens were analysed that were provided by J. Papier<sup>3</sup> and had been used by him in a study of 18-4-2 high-speed steels. The composition of this alloy was C 0.8%, W 18.8%, Cr 4.4%, V 1.9%.

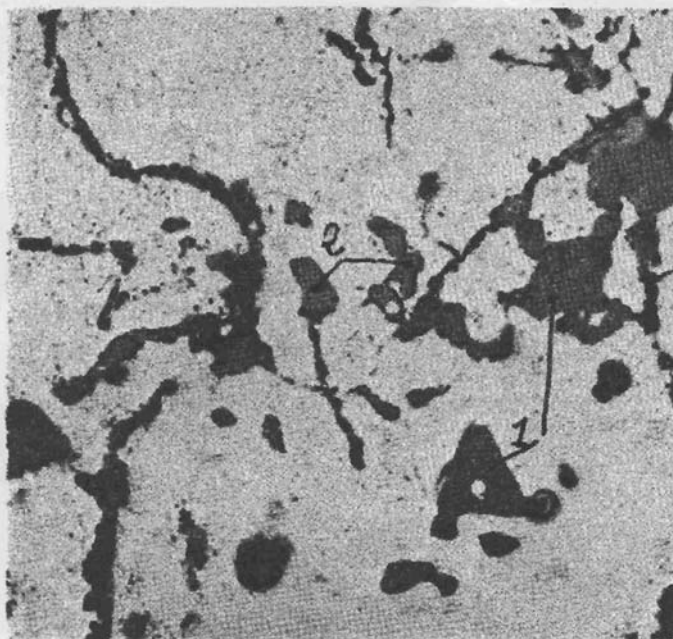
An interesting point is that in this case the micro-analyser can be used for direct analysis of the matrix while in the ordinary method involving electrolytic extraction of carbides, the composition of the matrix is determined by difference.

The specimens were studied after annealing at 1300° and 1050° C; after the first treatment, the carbide particles were fairly large (5μ approx.), while in the second case their dimensions were at the limit of the resolving power of the instrument. Table VI presents the proportions of Fe, W, and Cr in the complex tungsten carbides and the matrix; no figures are available for vanadium carbides and this should be the subject of further investigation.

In an Ni-Cr-Co turbine-blade austenitic steel, containing in addition a few per cent of Mo, W, and Nb, micrographs revealed minute grains of precipitated carbide; analysis reveals that these carbides contain only niobium, this element being absent in the matrix. It may be noted in passing that the element can be identified immediately as niobium and not tantalum.

**Segregation in an Overheated Steel**

Plateau, Duflo, and Crussard,<sup>4</sup> after etching a



1: 'mouse-grey' sulphide; 2: 'grey-black' sulphide  
**Fig. 6—Sulphides formed in the skin on cast iron and mechanically polished** × 480

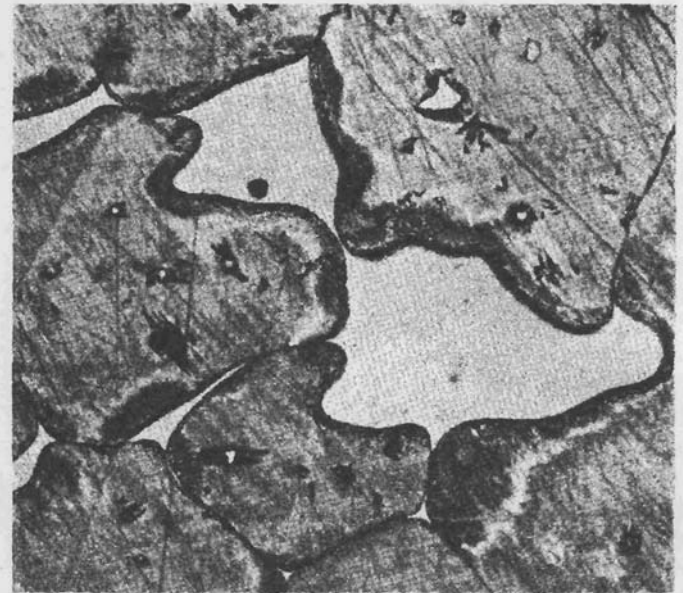


**Fig. 7—Hypereutectoid Cr steel, heated to 1160° C and quenched at 0° C. Austenite and ledeburite. Etched with Beaujard's reagent** × 340

hypereutectoid Cr steel overheated at 1160° C with Hall's reagent, observed coloured aureoles surrounding patches of ledeburite, indicating heterogeneity of chromium in the austenite. According to previous experiments on the diffusion of chromium in this steel, followed by etching with the same reagent, these aureoles are due to chromium enrichment. To confirm this conclusion by direct analysis, a study was made of the same steel, having the following composition: C 2.04%, Cr 2.86%, Si 0.2%, Mn 0.37%. This steel was austenitized for 6 h at 1100° C to increase the grain size, then heated for 15 min at 1160° C, and finally quenched in ice-water. After etching with Beaujard's reagent,<sup>5</sup> aureoles differing in colour from austenite are observed around areas of ledeburite (Fig. 7). Table VII shows the results of determination of Cr at various distances *d* from the ledeburite.

An enrichment of chromium of about 40% relative value will be observed in a zone of 15μ. It is interesting that this rather surprising result is confirmed by the microprobe.

**Iron-Chromium Alloys**

Following Pomey's work<sup>6</sup> on the transformation in Fe-Cr alloys, the present authors have found that in a pure 45% Cr alloy the amounts of Fe and Cr in the α- and σ-phases (σ-phase formed by cold-working) are equal; the transformation is diffusionless.

In less pure alloys, complex carbides of iron and

**Table VI**  
**ANALYSES OF TUNGSTEN CARBIDES**

Temperature of Austenitization	Phase	Fe	W	Cr	Total
1300° C	matrix	84.5	8.5	5	98
	carbide	31.5	60	3	94.5
1050° C	matrix	87.5	5.5	5	98
	carbide	31.5	56	3	90.5

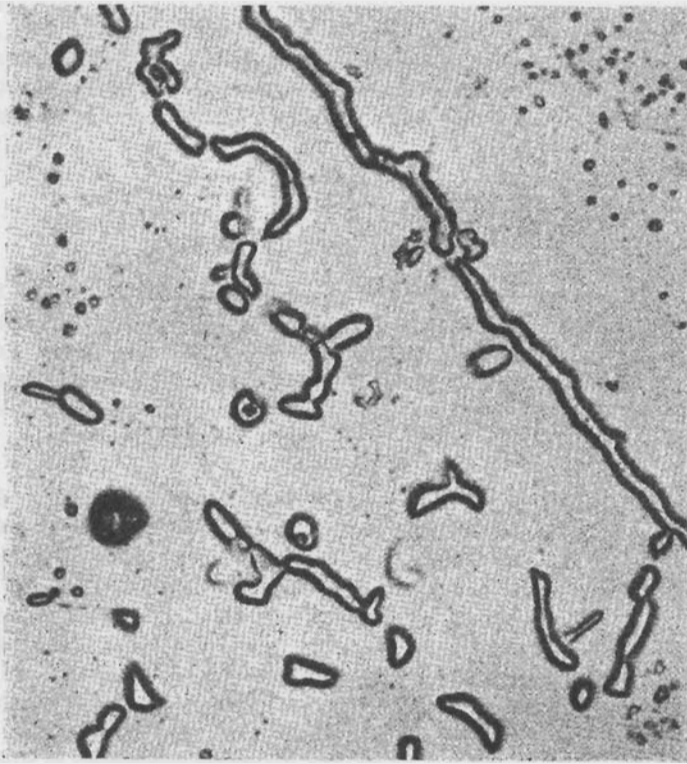


Fig. 8—Fe-30% Cr alloy, annealed at 1050° C. Ferrite and carbides. Electro-polished  $\times 710$

chromium can be formed by soaking at 1050° C; these carbides do not redissolve until the temperature reaches 1200° C. In a 30% Cr alloy annealed at 1050° C (Fig. 8), the parent metal is seen to be slightly depleted in Cr (28.5% Cr) and, near to the carbides, over a range of 4–5 $\mu$ , the Cr content falls to 26%. Analysis reveals 59% Cr and 31% Fe in the carbides, which are therefore probably of the formula  $M_7C_3$ .

This example illustrates the ease with which the contents in metal elements of phases in equilibrium can be determined with the microanalyser.

#### DIFFUSION PROBLEMS

The microanalyser is the best instrument for determining diffusion curves between two metals or alloys at high temperature; these curves can be plotted rapidly and with great accuracy.

A study of U-Zr interdiffusion is now being made in collaboration with the French Commissariat of Atomic Energy. At very high temperature, continuous diffusion curves are obtained, since diffusion occurs in a homogeneous phase; hence diffusion coefficients can be determined, with their concentration variations and heats of activation. At lower temperatures, there is multiphase diffusion and discontinuities on the diffusion curves enable measurements of solubilities to be made.

Table VII  
CHROMIUM DETERMINATION

		Example 1					
$d, \mu$		60	30	10	5	2	
Cr, %		2.35	2.6	2.7	3.15	3.5	
		Example 2					
$d, \mu$		60	30	20	10	6	3
Cr, %		2.3	2.3	2.35	2.9	3.1	3.4

#### Iron-Copper Diffusion

The authors have studied a series of specimens prepared by M. Sirca of the Ljubljana Institute of Metallography,\* in which, during diffusion, the copper or the copper alloy used is liquid, the iron being in the form of a crucible.<sup>7</sup>

The diffusion zones are fairly narrow, about 10 $\mu$  in certain cases, which makes it difficult to obtain precise diffusion curves. But in all cases, even when it has not been possible to obtain quantitative results such as values of diffusion coefficients, local analysis with the microanalyser has given interesting results. Three examples are given to illustrate this.

*Diffusion of Fe-Cu for 16 h at 1100° C (Fig. 9)*—Diffusion proceeds mainly along grain boundaries. After diffusion, each grain is surrounded by a succession of differently coloured aureoles. It has been possible to prove that these do not correspond to the formation of any particular phase. After a considerable discontinuity at the Fe/Cu interface, the copper content decreases regularly and progressively from 10% to less than 0.3% at the centres of the grains. The widest diffusion bands (those most oblique to the plane of the grain boundary) do not exceed 30–40 $\mu$ .

*Diffusion of Fe/Cu-P (2%) alloy for 96 h at 950° C*—In this case the diffusion is frontal. Three zones are observed in the iron (Fig. 10): a strongly attacked zone *A*, a zone of basaltic crystals *B*, and a zone of iron crystals of normal appearance *C*. The well-defined interfaces between these zones do not correspond to a marked discontinuity in the copper content; the variation in copper content is continuous, but the solubility of copper in iron is considerably lower than

\* M. Sirca is completing at IRSID research for a thesis, begun at Ljubljana, on the interdiffusion of iron and copper in the presence of a third element. He kindly provided the authors with some of his specimens.

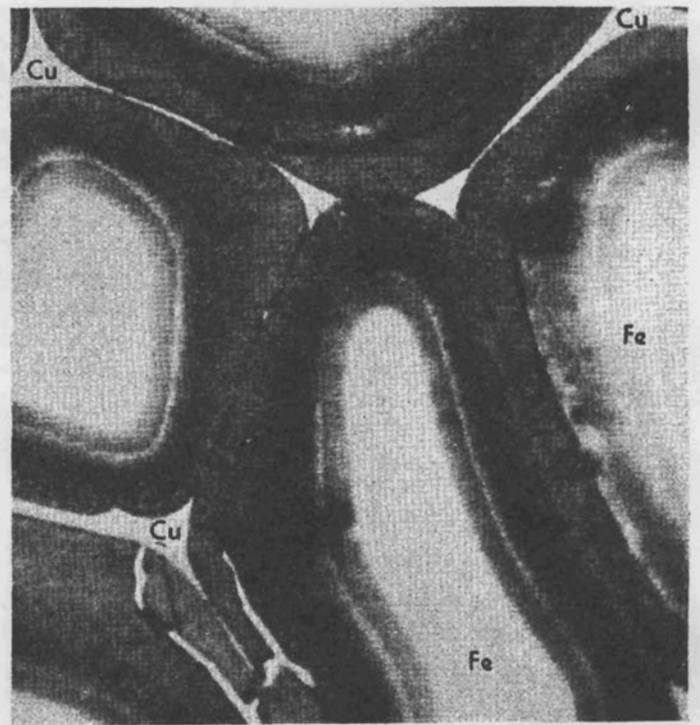


Fig. 9—Diffusion of Cu into Fe at 1100° C for 82 h. Etched with nital. (Grain-boundary diffusion of Cu and aureoles in the Fe grains)  $\times 350$

in the preceding case—not more than 4% of copper in zone A. In zone B a slight systematic enrichment was found across the grain boundaries. The distances, measured on either side of the boundary, are:

$d, \mu$	Example 1	Cu, %	Example 2
-5	1.7		1.8
	1.8		1.85
	1.85		2
+5	1.7		1.7

In copper, greyish-blue areas can be seen, probably consisting of a Fe-Cu-P eutectic formed on cooling; but there was depletion in Cu and enrichment in Fe in these areas as the Fe/Cu interface is approached. These distances, measured from the interface, were:

$d, \mu$	200-300	100-200	50	25	5
Cu, %	1.8-2.5	1-1.5	1	0.6	0.3

The three last measurements are made on the same area at three points approaching the Fe/Cu interface.

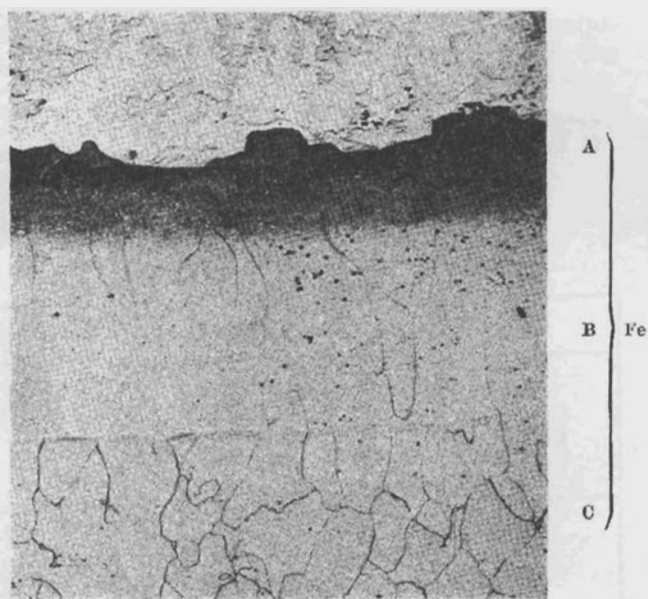
*Diffusion of Fe/Cu-Sb (2.5%) alloy for 64 h at 1100°*—In this case diffusion again occurs along grain boundaries. In each grain aureoles concentric with the boundaries are observed. In particular, there is a blue aureole (see Fig. 11). It was not possible to determine Sb contents, but only those of Fe and Cu.

Progressive segregation of Cu is observed as the grain is traversed from its centre to its boundary, but this time there is a discontinuity in passing into the blue zone. The copper content at the centre of the grain is at the limit of detection (0.1-0.2%?), and increases continuously to 1% at the boundary of the blue zone; there it jumps suddenly to 2%. In this zone it varies continuously, as far as it is possible to measure the variation in a zone about 12 $\mu$  wide, from 2% to 3%. On leaving this zone the Cu content increases to 4% and continues to increase to about 9%.

Thus the presence of three Cu-Fe-Sb phases has been demonstrated, which can only be identified with certainty by antimony determinations.

**CONCLUSIONS**

The few examples presented in the paper give only a faint idea of the possible applications of the micro-



At top: Cu + Fe-Cu-P eutectic  
**Fig. 10—Diffusion of Cu-P alloy into iron (frontal diffusion). Etched with nital**  $\times 70$

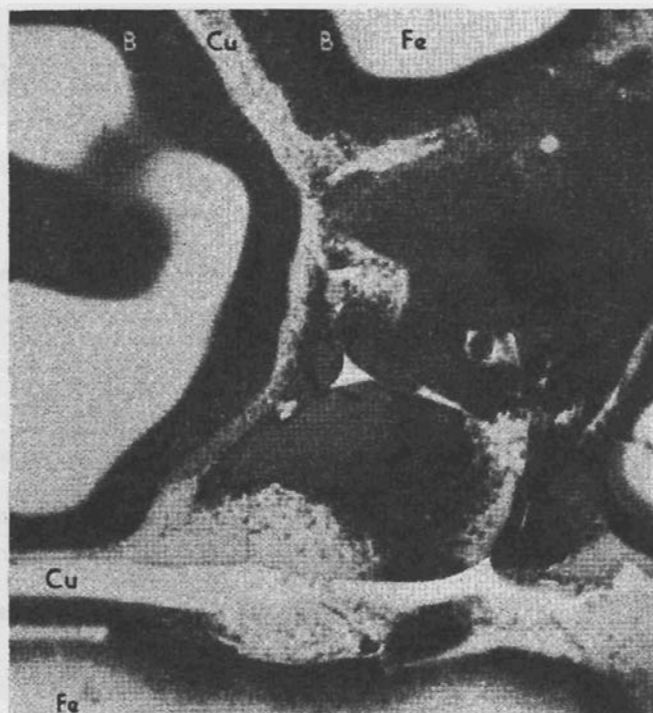


**Fig. 11—Diffusion of Cu-Sb alloy into Fe: grain boundary diffusion of Cu and aureoles in the Fe grains. At B aureole coloured blue by the etchant**  $\times 350$

analyser. They are the result of only two months' work, which in itself indicates how rapid and effective this new instrument is.

Used alone, the instrument's field of application is quite wide but, when used in conjunction with a method for revealing the distribution of elements with which it cannot cope (light elements like carbon, nitrogen, and oxygen, or elements in concentrations too low, such as P and S in steels), one may expect extremely interesting results concerning the solid-state interaction of certain metallic elements with the non-metals always present in alloys.

Another possible application of the microanalyser which has not yet been explored at IRSID is local crystal analysis by Kossel diagrams. Castaing<sup>1</sup> has been able to obtain such diagrams, which permit the crystal study of a region of about 5 $\mu$  radius, in which Kossel lines are produced.

Thus, used only for elementary and crystal analysis, or in combination with complementary methods (e.g. autoradiography), the microanalyser is capable of producing great advances in knowledge of the structure of metallurgical products.

**References**

1. R. CASTAING: Thesis, 1951, *ONERA Publication No. 55; Laboratoires (1956) No. 17*; R. CASTAING and J. DESCAMPS: *J. Phys. Radium*, 1955, vol. 16, pp. 304-317.
2. W. BETTERIDGE and R. S. SHARPE: *J. Iron Steel Inst.*, 1948, vol. 158, pp. 185-191.
3. J. PAPIER: *Rev. Mét.*, 1954, vol. 51, pp. 723-734.
4. J. PLATEAU, J. DUFLLOT, and C. CRUSSARD: *Rev. Mét.*, 1952, vol. 49, pp. 815-833.
5. L. BEAUJARD: *Rev. Mét.*, 1952, vol. 49, pp. 531-538.
6. G. POMEY: Thesis, 1955, *IRSID Publication A117*.
7. M. ZUMER and F. SIRCA: *Rudarsko-Metalurski Zbornik*, 1951, No. 1, p. 25; G. CIZERON and F. SIRCA: *Métaux-Corrosion Indust.*, 1956.